MO suffers significant changes (i.e. 12.04 eV in (H)(OEt)–Os_3 and 13.00 eV in (H)(Cl)–Os_3) according to the nature of the bridgehead atom.

Conclusion

The cluster derivatives reported in this study are probably the most complicated molecular systems so far studied by gas-phase PES. In our opinion, this study represents a challenge to the PE technique, from both the experimental and the interpretative points of view.

In spite of the high molecular complexity (about 15–20 MOs in the higher valence region), a qualitative discussion of the spectral data is possible on the basis of molecular orbitals that predominantly represent Os′–Os bonds, t_{2g}-like nonbonding pairs, or (μ-X)(μ-Y)Os_2 bridge bonds. In this respect the use of the He II ionizing source was of crucial importance in order to discern between bands relating to MOs having high metal "d" contribution and those mainly localized on the bridging heteroatoms.

The most interesting result deriving from this study is the similarity found between the PE spectra of $(H)_2$–Os_3, (H)(Y)–Os_3, and $(Y)_2$–Os_3 derivatives, which points to very similar bonding schemes. This would imply, in contrast to the simple EAN arguments, that there is not a net direct interaction between the bridged Os atoms in either case, but it allows the existence of a weak extra source of Os–Os interaction via the t_{2g}-like set that progressively reduces its importance on going from $(H)_2$–Os_3 to (H)(Y)–Os_3 and $(Y)_2$–Os_3. In our opinion, the present data support the "t_{2g}–t_{2g}" bond theory proposed by Sherwood and Hall[6] for $(H)_2$–Os_3. Furthermore, the experimental data clearly show that the bridge-bonding MOs are essentially composed of the AOs of the bridging atoms with their typical IEs.

Acknowledgment. We thank the Consiglio Nazionale dell Ricerche (CNR, Rome) for generous financial support of this study and Johnson Matthey Ltd. for a loan of OsO_4. Technical assistance of O. Lana is also gratefully acknowledged.

Registry No. $(H)_2Os_3(CO)_{10}$, 41766-80-7; $(H)(SEt)Os_3(CO)_{10}$, 23733-18-8; (H)(S-*i*-Bu)$Os_3(CO)_{10}$, 87569-04-8; (H)(S-*t*-Bu)$Os_3(CO)_{10}$, 59088-69-6; $(H)(OEt)Os_3(CO)_{10}$, 64489-41-4; $(OEt)_2Os_3(CO)_{10}$, 64387-08-2; $(H)(Cl)Os_3(CO)_{10}$, 12557-93-6; $(Cl)_2Os_3(CO)_{10}$, 28109-18-4; $(Br)_2Os_3(CO)_{10}$, 28109-19-5.

Contribution from the Departments of Chemistry, University of California, Riverside, California 92521, and University of California, San Diego, La Jolla, California 92093

Redox Chemistry of Iron Tetraphenylporphyrin, Imidazolate-Chelated Protoheme, and Thiolate-Chelated Protoheme and of Their Iron(II)–Superoxide Adducts in Dimethyl Sulfoxide

STEPHEN E. JONES, G. SUSAN SRIVATSA, DONALD T. SAWYER,* TEDDY G. TRAYLOR, and TERRY C. MINCEY

Received January 27, 1983

Cyclic voltammetry, controlled-potential coulometry, and UV–visible spectroscopy have been used to characterize the redox reactions in dimethyl sulfoxide of iron(III) *meso*-tetraphenylporphyrin, iron(III) protohemin monomethyl ester mono-(3-(1-imidazolyl)propyl)amide, and iron(III) protohemin monomethyl ester mono(3-(benzoylmercapto)propyl)amide and of the iron(II) thiolate that results from reduction and hydrolysis by addition of OH^-. All of these iron–porphyrin systems exhibit three reduction peaks [Fe(III)/Fe(II), Por/$Por^-\cdot$, and $Por^-\cdot/Por^{2-}$]; the last two are identical with those observed for zinc(II) *meso*-tetraphenylporphyrin. Addition of superoxide ion to the iron(II) state of these porphyrins yields an Fe(III)–(O_2^{2-}) adduct. In the case of iron(II) thiolated protoheme, the resulting peroxide complex may provide an effective model for the monooxygenase mechanism of cytochrome P-450.

Hemoproteins provide a variety of biological functions via their iron–porphyrin centers.[1] These include dioxygen transport by the myoglobin–hemoglobin proteins,[2-4] monooxygenase catalysis by cytochrome P-450,[5,6] four-electron reduction of dioxygen by cytochrome oxidase,[7-10] and the disproportionation and activation of peroxides by the catalase/peroxidase proteins.[11,12] The reversible binding of dioxygen occurs at a five-coordinate iron(II)–protoporphyrin molecule with its axial position occupied by an imidazole.[3] Cytochrome P-450 also has a five-coordinate structure, but as an iron(III) porphyrin with the axial position occupied by a thiolate anion.[5,13] Peroxidases such as horseradish peroxidase and cytochrome *c* peroxidase contain iron(III) protoporphyrin IX with the fifth ligand position on the iron occupied by an imidazole.[14]

The most extensively studied model systems involve the iron tetraphenylmeso- and octaethylprotoporphyrin complexes.

---

* To whom correspondence should be addressed at the University of California, Riverside.

(1) James, B. R. "The Porphyrins"; Dolphin, D., Ed.; Academic Press: New York, 1978; Vol. 5; p 205, 253.

(2) Rifkin, J. M. "Inorganic Biochemistry"; Eichhorn, G., Ed.; Elsevier: Amsterdam, 1973; Vol. 2, p 832.

(3) Antonini, E.; Bennori, M. "Hemoglobin and Myoglobin in Their Reactions with Ligands"; North-Holland Publishing Co.: Amsterdam, 1971.

(4) Collman, J. P. *Acc. Chem. Res.* **1977**, *10*, 265.

(5) White, R. E.; Coon, M. J. *Ann. Rev. Biochem.* **1980**, *49*, 315 (and ref 1–15 therein).

(6) Collman, J. P.; Sorrell, T. N.; Dawson, J. H.; Trudell, J. R.; Bunnenberg, E.; Djerrasi, C. *Proc. Natl. Acad. Sci. U.S.A.* **1976**, *73*, 6.

(7) Hayaishi, O., Ed. "Molecular Oxygen in Biology"; North-Holland Publishing Co.: Amsterdam, 1974.

(8) Bennett, L. E. *Prog. Inorg. Chem.* **1973**, *18*, 1.

(9) Wharton, D. C. "Inorganic Biochemistry"; Eichhorn, G., Ed.; Elsevier: Amsterdam, 1973; Vol. 2.

(10) Wilson, D. F.; Erecinska, M. "The Porphyrins"; Dolphin, D., Ed.; Academic Press: New York, 1979; Vol. 7, p. 1.

(11) Hewson, W. D.; Hager, L. P. "The Porphyrins"; Dolphin, D., Ed.; Academic Press: New York, 1979; Vol. 7.

(12) Dunford, H. B.; Stillman, J. S. *Coord. Chem. Rev.* **1976**, *19*, 187.

(13) Dawson, J. H.; Cramer, S. P. *FEBS Lett.* **1978**, *88*, 127.

(14) Yonetani, J.; Yamamoto, H.; Erman, J. E.; Leigh, J. S., Jr.; Reed, G. H. *J. Biol. Chem.* **1972**, *247*, 2447.

0020-1669/83/1322-3903$01.50/0

Several iron(II) porphyrins that reversibly bind dioxygen have been synthesized and characterized.[4,15-21] Additional studies have been directed to the reaction of the superoxide ion (O_2^-) with synthetic iron(III) porphyrins in aqueous[22-24] and nonaqueous[25-28] media. For all of these systems O_2^- appears to reduce the iron(III) porphyrin:

$$\mathrm{Fe^{III}(Por)^+ + O_2^- \rightarrow Fe^{II}(Por) + O_2} \tag{1}$$

In the absence of a proton source, dioxygen does not appear to react via electron transfer with $\mathrm{Fe^{II}(Por)}$. That is, reaction 1 is not reversible and the reversible binding of dioxygen by iron(II)–porphyrin complexes[21,29] must involve an adduct without significant intramolecular electron transfer.

Addition of excess O_2^- to $\mathrm{Fe^{III}(Por)^+}$ results in formation of an apparent iron(III) peroxide[25,29] by oxidative coupling with the $\mathrm{Fe^{II}(Por)}$ that results from reaction 1

$$\mathrm{Fe^{II}(Por) + O_2^- \rightarrow Fe^{III}(Por)(O_2)^-} \tag{2}$$

This reaction chemistry has been studied by visible,[25-27] ESR,[25,27] NMR,[30,31] IR, and resonance Raman spectroscopy[25,32] and by cyclic voltammetry.[27] Although there have been several electrochemical studies of heme model systems,[33-37] a detailed redox characterization of their dioxygen and superoxide adducts in aprotic media has not been undertaken previously.

The most successful models for hemoproteins involve either protected hemes or chelated hemes.[38,40] Although several elegant hemoprotein models with a protected heme have been prepared that form stable dioxygen complexes in solution,[4,41-46] models with an attached protective chelate function exhibit reversible dioxygen binding that is closer to that of myoglobin and hemoglobin.[4,18,31,39,47,48]

Reasonable models for cytochrome P-450 involve an axial sulfide ligand[6,49-51] and include one with a covalently attached thiolate ligand on the porphyrin ring.[49] Because of the tendency of iron(III) to oxidize the thiolate function (eq 3),[52] a

$$\mathrm{2(hemin)(1+) + 2RSH \rightleftharpoons 2(heme) + RSSR + 2H^+} \tag{3}$$

protected thiol ester has been synthesized. The thiolate can be released by base hydrolysis after the iron(III) center is reduced by dithionite ($S_2O_4^{2-}$) (eq 4).

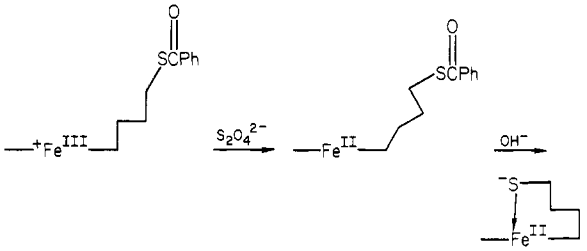

(4)

To understand the interaction of the dioxygen species with heme proteins and their redox behavior, a coordinated study of superoxide adducts of several iron–porphyrin model complexes has been undertaken. Because the iron center, the porphyrin ring system, and dioxygen are all electroactive, electrochemical measurements provide a unique means to probe and to characterize these systems. The present investigation summarizes the results of electrochemical and spectroscopic studies of the redox chemistry of iron–tetraphenylmesoporphyrin and two iron-chelated protoheme (im-

---

(15) Reed, C. A. *Met. Ions Biol. Syst.* **1978**, *7*, 277.

(16) Chin, D.-H.; Del Gaudio, J.; LaMar, G. N.; Balch, A. L. *J. Am. Chem. Soc.* **1977**, *99*, 5486.

(17) Fuchman, W. H.; Barlow, C. H.; Wallace, W. J.; Caughey, W. S. *Biochem. Biophys. Res. Commun.* **1974**, *61*, 635.

(18) Traylor, T. G.; Berzimis, A. P. *Proc. Natl. Acad. Sci. U.S.A.* **1980**, *77*, 3171.

(19) Brinigar, W. S.; Chang, C. K. *J. Am. Chem. Soc.* **1974**, *96*, 5595.

(20) Anderson. D. L.; Weschlier, C. J.; Basolo, F. *J. Am. Chem. Soc.* **1980**, *96*, 5599.

(21) Almog, J.; Baldwin, J. E.; Dyer, R. L.; Huff, J.; Wilkerson, C. J. *J. Am. Chem. Soc.* **1980**, *96*, 5600.

(22) Pasternak, R. F.; Halliwell, B. *J. Am. Chem. Soc.* **1979**, *101*, 1026.

(23) Bettelheim, A.; Kuwana, T. *Anal. Chem.* **1979**, *51*, 2257.

(24) Winterbourn, C. C.; McGrath, G.; Carrell, R. W. *Biochem. J.* **1976**, *155*, 493.

(25) McCandlish, E.; Miksztal, A. R.; Nappa, M.; Sprenger, A. Q.; Valentine, J. S.; Strong, J. D.; Spiro, T. G. *J. Am. Chem. Soc.* **1980**, *102*, 4268.

(26) Hill, H. A. O.; Turner, D. R. *Biochem. Biophys. Res. Commun.* **1974**, *56*, 379.

(27) Welborn, C. H.; Dolphin, D.; James, B. R. *J. Am. Chem. Soc.* **1981**, *103*, 2869.

(28) Afanasen, I. B.; Prigoda, S. V.; Khenkin, A. M.; Shteinman, A. A. *Dokl. Akad. Nauk SSSR* **1977**, *236*, 902.

(29) Weschler, C. J.; Anderson, D. L.; Basolo, F. *J. Am. Chem. Soc.* **1975**, *97*, 6707.

(30) Chin, D.-H.; LaMar, G. N.; Balch, A. L. *J. Am. Chem. Soc.* **1980**, *102*, 4344.

(31) Traylor, T. G.; Chang, C. K.; Geibel, T.; Berzinis, A.; Mincey, T.; Cannon, J. *J. Am. Chem. Soc.* **1979**, *101*, 6716.

(32) Walters, M. A.; Spiro, T. G.; Suslick, K. S.; Collman, J. P. *J. Am. Chem. Soc.* **1980**, *102*, 6857.

(33) Davis, D. G.; Orleron, D. J. *Anal. Chem.* **1966**, *38*, 179.

(34) Lexa, D.; Momenteau, M.; Mispeltier, J. *Biochim. Biophys. Acta* **1974**, *338*, 151.

(35) (a) Kadish, K. M.; Bottomley, L. A. *Inorg. Chem.* **1980**, *19*, 832. (b) Kadish, K. M.; Bottomley, L. A. *J. Am. Chem. Soc.* **1977**, *99*, 2380. (c) Kadish, K. M.; Bottomley, L. A. *Inorg. Chem.* **1980**, *19*, 382.

(36) Kadish, K. M.; Larson, G.; Lexa, D.; Momenteau, M. *J. Am. Chem. Soc.* **1975**, *97*, 282.

(37) (a) Phillippi, M. A.; Goff, H. M. *J. Am. Chem. Soc.* **1979**, *101*, 7641. (b) Phillippi, M. A.; Shimonra, E. T.; Goff, H. M. *Inorg. Chem.* **1981**, *20*, 1322.

(38) Collman, J. P.; Brauman, J. I.; Doxsee, K. M.; Holbert, T. R.; Bunnenberg, E.; Linden, R. E.; LaMar, G. N.; Del Gaudio, J.; Lang, G.; Spartalian, K. *J. Am. Chem. Soc.* **1980**, *102*, 4182.

(39) Traylor, T. G.; Campbell, P.; Tsuchiya, S. *J. Am. Chem. Soc.* **1979**, *101*, 4749.

(40) (a) Budge, J. R.; Ellis, P. E.; Jones, R. D.; Linard, J. E.; Basolo, F.; Baldwin, J. E.; Dyer, R. L. *J. Am. Chem. Soc.* **1979**, *101*, 4760. (b) Budge, J. R.; Ellis, P. E.; Jones, R. D.; Linard, J. E.; Szymanski, T.; Basolo, F.; Baldwin, J. E.; Dyer, R. L. *J. Am. Chem. Soc.* **1979**, *101*, 4763.

(41) Diekmann, H.; Chang, C. K.; Traylor, T. G. *J. Am. Chem. Soc.* **1971**, *93*, 4068.

(42) Almog, J.; Baldwin, J. E.; Dyer, R. L.; Peters, J. *J. Am. Chem. Soc.* **1975**, *97*, 226. (b) Almog, J.; Baldwin, J. E.; Huff, J. *J. Am. Chem. Soc.* **1975**, *97*, 227. (c) Baldwin, J. E.; Klose, T.; Peters, M. *J. Chem. Soc., Chem. Commun.* **1976**, 881.

(43) (a) Collman, J. P.; Gagnê, R. R.; Halbert, T. R.; Marchon, J. C.; Reed, C. A. *J. Am. Chem. Soc.* **1973**, *95*, 7868. (b) Collman, J. P.; Brauman, J. I.; Doxsee, K. M.; Halbert, T. R.; Suslick, K. S. *Proc. Natl. Acad. Sci. U.S.A.* **1978**, *75*, 564. (c) Collman, J. P. *Acc. Chem. Res.* **1977**, *10*, 265.

(44) Ogoshi, H.; Sugimoto, H.; Yoshida, F. *Hukusokan Kagaku Toronkai Koen Yoshisu, 8th* **1975**, 239; *Chem. Abstr.* **1975**, *84*, 164069.

(45) Chang. C. K. *J. Am. Chem. Soc.* **1977**, *99*, 2819.

(46) (a) Battersby, A. R.; Buckley, D. G.; Hartley, S. G.; Turnbull, M. D. *J. Chem. Soc., Chem. Commun.* **1976**, 879. (b) Battersby, A. R.; Hamilton, A. D. *Ibid.* **1980**, 117.

(47) (a) Chang, C. K.; Traylor, T. G. *Proc. Natl. Acad. Sci U.S.A.* **1973**, *70*, 2647. (b) Geibel, J.; Chang, C. K.; Traylor, T. G. *J. Am. Chem. Soc.* **1975**, *97*, 5924.

(48) Traylor, T. G.; White, D. K.; Campbell, D. H.; Berzinis, A. P. *J. Am. Chem. Soc.* **1981**, *103*, 4932.

(49) (a) Traylor, T. G. *Acc. Chem. Res.* **1981**, *14*, 102. (b) Traylor, T. G.; Mincey, T. C. *Acta Biol. Med. Ger.* **1979**, *38*, 351. (c) Traylor, T. G.; Mincey, T. C.; Berzinis, A. P. *J. Am. Chem. Soc.* **1981**, *103*, 7084.

(50) Stern, J. O.; Peisach, J. *J. Biol. Chem.* **1974**, *249*, 7495.

(51) Chang, C. K.; Dolphin, D. *Proc. Natl. Acad. Sci. U.S.A.* **1976**, *73*, 3338.

(52) Capozzi, G.; Modena, C. In "The Chemistry of the Thiol Group"; Patai, S., Ed.; Wiley: New York, 1974; pp 669–689.

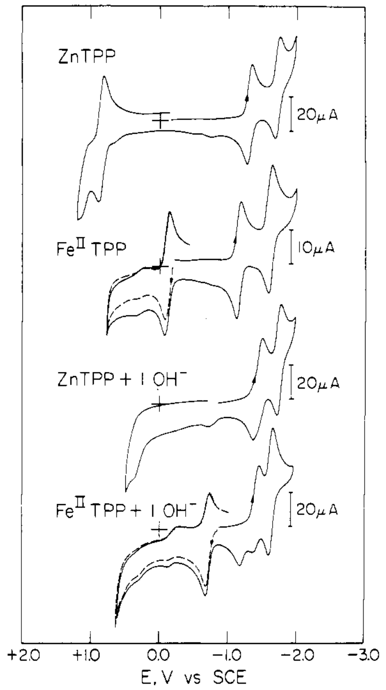

Figure 1. Cyclic voltammograms in dimethyl sulfoxide (Me_2SO) (0.1 M tetraethylammonium perchlorate (TEAP)) of 1.40 mM (*meso*-tetraphenylporphinato)zinc(II) ($Zn^{II}TPP$), 0.62 mM (*meso*-tetraphenylporphinato)iron(II) ($Fe^{II}TPP$), 2.10 mM $Zn^{II}TPP$ plus 2.35 mM tetraethylammonium hydroxide ((TEA)OH), and 1.32 mM $Fe^{II}TPP$ plus 1.32 mM (TEA)OH (scan rate 0.1 V s^{-1}).

idazole and thiolate)[31,49] complexes in dimethyl sulfoxide. The effects of O_2, O_2^-, and OH^- on these redox processes have been determined. A primary goal has been to ascertain if an axial thiolate provides a route to the transient formation of an activated dioxygen adduct that is relevant to cytochrome P-450 chemistry.

Experimental Section

Equipment. A three-electrode potentiostat (Princeton Applied Research Model 173/175/179 with universal programmer and digital coulometer) was used for the cyclic voltammetric and controlled-potential electrolysis experiments. Cyclic voltammograms were recorded on a Houston Instrument Series 100 X-Y recorder.

A Bioanalytical Systems microcell assembly was adapted to use a platinum-wire working electrode, a platinum-flag auxiliary electrode, and an Ag/AgCl reference electrode filled with aqueous tetramethylammonium chloride solution and adjusted to 0.000 V vs. SCE.[53] The latter was contained in a Pyrex tube with a soft-glass cracked tip; this electrode was placed inside a luggin capillary that contained the aprotic electrolyte solution. For controlled-potential electrolysis, a platinum-mesh working electrode was employed. The cell was closed with a Teflon cap that included holes for deaeration by high-purity argon and for sample introduction.

Cary Model 17D and Model 219 spectrophotometers were used for the UV–visible spectrophotometric measurements. The magnetic susceptibility measurements were made with a Varian EM-390 NMR spectrometer by the method of Evans[54] as modified by Rettig[55] and made use of the paramagnetic shift of the methyl protons of the solvent. The susceptibilities for solid samples were determined by the Faraday method on a Cahn Model 2000 balance.

Reagents. Dimethyl sulfoxide (Me_2SO), *N,N*-dimethylformamide (DMF), and pyridine (all Burdick and Jackson Laboratories "distilled in glass") were used as received for the studies in the solution phase. Tetraethylammonium perchlorate (TEAP) (G. Frederick Smith Co.) was used as the supporting electrolyte in the electrochemical studies.

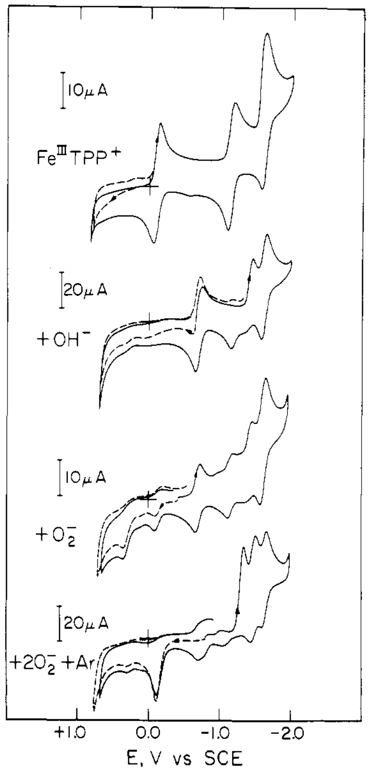

Figure 2. Cyclic voltammograms in Me_2SO (0.1 M TEAP) of 1.18 mM (*meso*-tetraphenylporphinato)iron(III) ($Fe^{III}TPP^+$), 1.02 mM $Fe^{III}TPP^+$ plus 2.05 mM (TEA)OH, 0.71 mM $Fe^{III}TPP^+$ plus 0.78 mM tetramethylammonium superoxide ($(TMA)O_2$), and 1.21 mM $Fe^{II}TPP$ plus 1.20 mM $(TMA)O_2$ (scan rate 0.1 V s^{-1}).

(*meso*-Tetraphenylporphinatoiron(III) chloride ($[Fe^{III}TPP]Cl$), (*μ*-oxo)bis[(*meso*-tetraphenylporphinato)iron(III)]($[Fe^{III}TPP]_2O$), and (*meso*-tetraphenylporphinato)zinc(II) ($Zn^{II}TPP$) were obtained from Strem Chemicals. The protohemin monomethyl ester mono(3-(1–imidazolyl)propyl)amide ($[Fe^{III}PrH(ME(Im)]Cl$)[31] and protohemin monomethyl ester mono(3-(benzoylmercapto)propyl)amide ($[Fe^{III}PrH(ME)\ (SC(O)Ph)]Cl$)[49] were prepared and characterized by previous methods. Tetraethylammonium hydroxide ((TEA)OH) was obtained from Eastman Kodak Co. as a 25% solution in methanol (0.934 M OH^- on the basis of titration). Tetramethylammonium superoxide [$(Me_4N)O_2$] was prepared by combination of KO_2 and $(Me_4N)OH{\cdot}5H_2O$ and subsequent extraction in liquid ammonia.[56] After dissolution in Me_2SO the concentration of $(Me_4N)O_2$ was determined by cyclic voltammetry immediately prior to its use.[57]

The cyclic voltammograms were initiated at the rest potential of the solution, and all voltages are reported vs. SCE. All of the solutions contained 0.1 M tetraethylammonium perchlorate as a supporting electrolyte and were characterized at 24 ± 0.5 °C.

Results

Electrochemistry. Figure 1 illustrates the cyclic voltammetry for $Fe^{II}TPP$ and for $Zn^{II}TPP$ in Me_2SO. Addition of OH^- results in axial bonding of the respective metal centers (Figure 1c,d), as confirmed by the negative shifts of the first reduction peaks.

The cyclic voltammogram of $Fe^{III}TPP^+$ in Me_2SO (Figure 2) is substantially the same as it is in dimethylformamide (DMF).[36] Addition of 1 equiv of OH^- to $Fe^{III}TPP^+$ results in the cyclic voltammogram of Figure 2b, and the combination of 1 equiv of O_2^-/equiv of $Fe^{III}TPP^+$ results in the cyclic voltammogram of Figure 2c. This same voltammogram is obtained for a Me_2SO solution that contains 1 equiv of molecular oxygen and 1 equiv of $Fe^{II}TPP$. Addition of 2 equiv of O_2^- to $Fe^{III}TPP^+$ followed by deaeration with argon results

---

(53) Sawyer, D. T.; Roberts, J. L., Jr. In "Experimental Electrochemistry fore Chemists"; Wiley-Interscience: New York, 1974; p 144.

(54) Evans, D. F. *J. Chem. Soc.* **1959**, 2003.

(55) Rettig, M. F., private communication, University of California, Riverside, CA.

(56) McElroy, A. D.; Hashman, J. S. *Inorg. Chem.* **1964**, *3*, 1978.

(57) Sawyer, D. T.; Calderwood, T. S.; Yamaguchi, K.; Angelis, C. T. *Inorg. Chem.* **1983**, *22*, 2577.

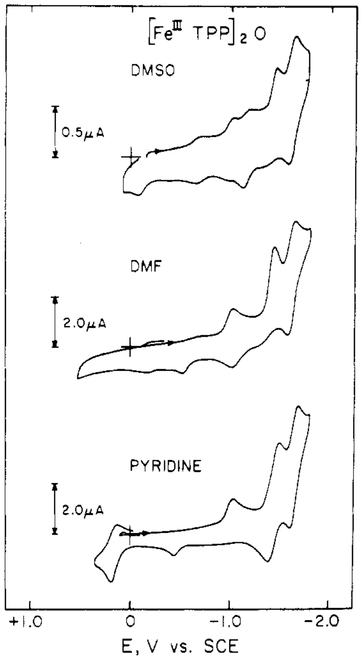

Figure 3. Cyclic voltammograms of (μ-oxo)bis[(*meso*-tetraphenylporphinato)iron(III)] ([Fe^{III}TPP]$_2$O) in dimethyl sulfoxide (0.05 mM), dimethylformamide (0.4 mM), and pyridine (0.4 mM) (scan rate 0.1 V s^{-1} at a Pt electrode (0.03 cm^2)). All solutions contained 0.1 M TEAP.

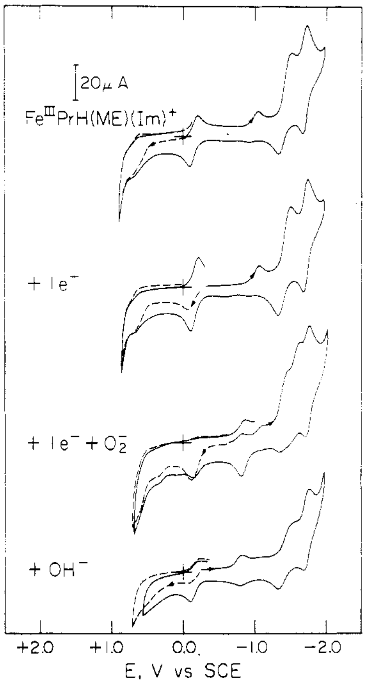

Figure 4. Cyclic voltammograms in Me$_2$SO (0.1 M TEAP) of 1.42 mM protohemin monomethyl ester mono(3-(1-imidazolyl)propyl)amide (Fe^{III}PrH(ME)(Im)$^+$), 1.42 mM Fe^{II}PrH(ME)(Im), 1.42 mM Fe^{II}PrH(ME)(Im) plus 1.39 mM (TMA)O$_2$, and 1.05 mM Fe^{III}PrH(ME)(Im) plus 1.08 mM (TEA)OH (scan rate 0.1 V s^{-1}).

in the cyclic voltammogram of Figure 2d. An identical voltammogram is observed for a Me$_2$SO solution that contains 1 equiv of O$_2^-$ and 1 equiv of Fe^{II}TPP.

The cyclic voltammograms for (μ-oxo)bis[(*meso*-tetraphenylporphinato)iron(III)] in Me$_2$SO, DMF, and pyridine solutions are illustrated in Figure 3. The electrochemistry in DMF is analogous to that of a previous study.[36] In Me$_2$SO the μ-oxo dimer is almost insoluble and appears to decompose; it is much more soluble in DMF and pyridine and gives a clean reduction peak at −1.0 V vs. SCE (one electron per dimer). There are no additional anodic peaks for the dimer in Me$_2$SO until the porphyrin-ring oxidations.

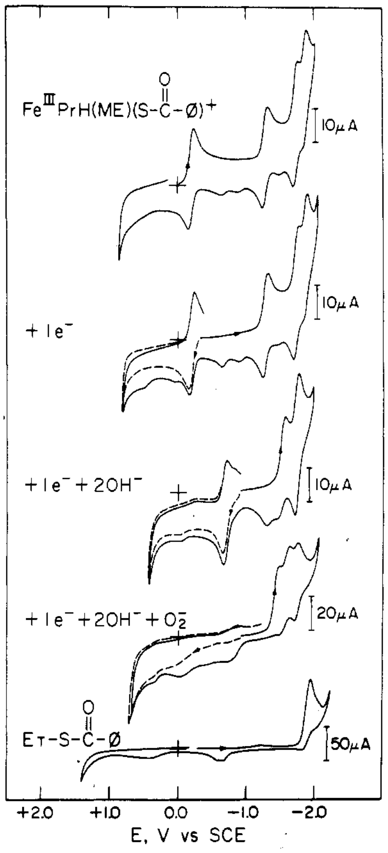

Figure 5. Cyclic voltammograms in Me$_2$SO (0.1 M TEAP) of 0.77 mM protohemin monomethyl ester mono(3-(benzoylmercapto)propyl)amide (Fe^{III}PrH(ME)(SC(O)Ph)$^+$), 0.77 mM Fe^{II}PrH(ME)(SC(O)Ph), 0.77 mM Fe^{II}PrH(ME)(SC(O)Ph) plus 1.51 mM (TEA)OH, 0.77 mM Fe^{II}PrH(ME)(SC(O)Ph) plus 1.51 mM (TEA)OH plus 0.80 mM (TMA)O$_2$, and 13.7 mM ethyl thiobenzoate (EtSC(O)Ph) (scan rate 0.1 V s^{-1}).

The cyclic voltammogram for the imidazolate-chelated protoheme, Fe^{III}PrH(ME)(Im)$^+$, is shown in Figure 4a. Its one-electron reduction product exhibits the same redox peak potentials for porphyrin ring reductions as the iron(III) complex. Addition of 1 equiv of O$_2^-$ to Fe^{II}PrH(ME)(Im) yields a product with the cyclic voltammogram shown in Figure 4c. Likewise, combination of 1 equiv of OH$^-$ to 1 equiv of Fe^{III}PrH(ME)(Im)$^+$ gives the cyclic voltammogram in Figure 4d.

The cyclic voltammogram in Me$_2$SO for the thio ester of the protoheme, Fe^{III}PrH(ME)(SC(O)Ph)$^+$, is illustrated in Figure 5a. The one-electron reduction product of Fe^{III}PrH(ME)(SC(O)Ph)$^+$ exhibits the electrochemistry illustrated by Figure 5b with the same porphyrin-ring reduction and oxidation peaks as for the case of the Fe(III) species. After electrochemical reduction to Fe^{II}PrH(ME)(SC(O)Ph), the addition of 2 equiv of OH$^-$ hydrolyzes the thio ester to the thiolate (Figure 5c); the latter appears to bind to an axial position of the iron center. Addition of 1 equiv of O$_2^-$ to the resulting solution yields an adduct with the cyclic voltammogram of Figure 5d. Figure 5e illustrates the cyclic voltammogram of ethyl thiobenzoate, EtSC(O)Ph, which indicates that the reduction peak at −1.89 V for Fe^{II}PrH(ME)(SC(O)Ph) is due to its thio ester protecting group.

Optical Spectra. The optical spectra for the various iron–porphyrin species in Me$_2$SO are summarized in Table I and are in accord with the published UV–visible spectra of Fe^{III}TPP(Me$_2$SO)$_2^+$,[58] Fe^{II}TPP(Me$_2$SO)$_2$,[25,58] Fe^{III}TPP-

Table I. UV-Visible Absorption Bands for the Various Porphyrin Complexes of Iron(III), Iron(II), and Zinc(II) and Their O_2^- and OH^- Adducts in Me_2SO (0.1 M TEAP)

compd	λ_{max}, nm (ϵ, mM^{-1} cm^{-1})		
	Soret	β	α
TPP: $Fe^{III}Cl$	413 (98.0)	493 (9.7) 528 (12.2)	648 (1.8) 688 (2.6)
$Fe^{III} + O_2^-$	413 (85.0) 426 (74.0)	527 (7.5) 569 (9.7)	610 (7.4)
$Fe^{III} + O_2^- + Ar$	413 (84.0) 426 (85.0)	527 (7.7) 569 (9.5)	610 (5.8)
Fe^{II}	408 (67.0) 428 (170.0)	529 (7.9) 567 (5.8)	608 (2.2)
$Fe^{II} + O_2$	408 (93.0) 426 (70.0)	529 (4.8) 567 (7.5)	608 (3.9)
$Fe^{II} + O_2^- + Ar$	417 (77.8) 436 (117.3)	566 (9.8)	609 (4.3)
$Fe^{III} + OH^- + Ar$	418 (112.4)	574 (8.4)	620 (5.5)
$Fe^{II} + OH^-$	415 (92.0) 436 (112.4)	570 (7.8)	619 (5.5)
PrH(ME)(Im): $Fe^{III}Cl$	404 (76.2)	565 (5.1)	615 (3.8)
$Fe^{III}Cl + OH^-$	401 (36.8) 426 (34.9)	558 (7.1)	585 (6.0)
Fe^{II}	424	526	556
$Fe^{II} + O_2^-$	403 (30.7) 422 (34.1)	524 (5.8)	555 (7.1)
PrH(ME)(SC(O)Ph): $Fe^{III}Cl$	404 (197.6)	492 (5.1)	624 (6.2)
$Fe^{III}Cl + OH^-$	398 (73.3) 435 (19.5)	563 (12.0)	585 (11.5)
Fe^{II}	422	520	555
$Fe^{II} + O_2^-$	399 (111.1)	565 (6.2)	593 (5.3)
$Fe^{II} + 2OH^-$	396 (114.8) 422 (84.1)	557 (9.1)	586 (7.2)
$Fe^{II} + 2OH^- + O_2^-$	401 (95.5) 433 (79.4)	560 (6.8)	609 (6.3)
$(Fe^{III}TPP)_2O$ (Me_2SO)	409	568	609
(DMF)	317 (24.1), 407 (81.5)	569 (7.7)	609 (4.4), 642 (2.1)
(py)	410 (107.4)	528 (5.3) 569 (9.3)	612 (4.7)
$Zn^{II}TPP$	427 (771.0)	520 (10.3) 559 (28.4)	598 (17.5)
$+OH^-$	426 (554.8) 435 (167.7)	520 (11.0) 559 (25.5)	599 (16.4)
$+O_2^-$	426 (523.1) 435 (211.5)	520 (11.2) 559 (25.4)	599 (16.9)

$(O_2^{2-})^-$,[25] $(Fe^{III}TPP)_2O$,[59] $Fe^{III}PrH(ME)^+$,[41] $Fe^{III}PrH(ME)(SC(O)Ph)^+$,[41] $Fe^{II}PrH(ME)(SC(O)Ph)$,[41] $Fe^{II}PrH(ME)(S^-)^-$,[41] $Zn^{II}TPP$,[60–62] $Zn^{II}TPP(OH)^-$,[62] and $Zn^{II}TPP(O_2^-)$.[62] The Fe(II) complexes have been formed by electrochemical reduction of the Fe(III) species in the absence of oxygen. The appearance of a red-shifted Soret band is characteristic of iron(II) porphyrins vs. their iron(III) counterparts. If molecular oxygen is allowed to diffuse into the cuvettes prior to running the samples, a split-Soret band appears with the peaks separated by about 20 nm. If molecular oxygen is bubbled through a solution of $Fe^{II}TPP$ in DMF, the visible spectrum slowly changes to that for the (μ-O)$(Fe^{III}TPP)_2$ complex. The UV–vis spectra of $Fe^{III}TPP^+$, $Fe^{II}TPP$, $(Fe^{III}TPP)_2O$, and the electrochemical one-electron-reduction product (at −1.4 V vs. SCE under N_2 atmosphere) in DMF are shown in Figure 6. The spectrum of this species exhibits a split-Soret band (λ_{max} 394 nm (ϵ 68.8 mM^{-1} cm^{-1}), λ_{max} 418 nm (ϵ 75.0 mM^{-1} cm^{-1})) and five bands in the visible region. (The stability of this species in dry, O_2^--free DMF was confirmed by electrochemical measurements; synthesis of stable solutions in Me_2SO was not possible.)

Addition of 1 equiv of $(Me_4N)O_2$ to $Fe^{III}TPP^+$ converts the latter to a dioxygen adduct, $Fe^{II}TPP(O_2)$ with a split-Soret band (λ_{max} 413 and 426 nm). Prolonged deaearation with argon is required to convert this split band to a single peak at 435 nm (equivalent to that for $Fe^{II}TPP$ plus O_2^-). When 2 or 3 equiv of $(Me_4N)O_2$ is added to $Fe^{III}TPP^+$, the same split-Soret band is observed. If the $Fe^{III}TPP^+$ complex is reduced electrochemically before 1 equiv of $(Me_4N)O_2$ is added, the spectrum for the $Fe^{III}TPP(O_2^{2-})$ complex ($Fe^{II}TPP + O_2^-$) is formed immediately. The addition of 1 equiv of OH^- to a solution of $Fe^{III}TPP^+$ causes the Soret band to shift to 418 nm from 413 nm. When 1 equiv of OH^- is added to $Fe^{II}TPP$, the Soret band becomes a doublet (λ_{max} 415 and 436 nm), and when 1 equiv of OH^- is added to $Zn^{II}TPP$, the Soret band also splits to give absorptions at 426 and 435 nm.

Electrochemical reduction of $Fe^{III}PrH(ME)(Im)^+$ to its Fe(II) analogue yields a product that has the same visible spectrum as that from dithionite reduction.[31] This also is true for the $Fe^{III}PrH(ME)(SC(O)Ph)$ complex and the subsequent deprotection of the mercaptide group with OH^-. Addition of $(Me_4N)O_2$ to the latter solution results in a red-shift of the Soret band to 433 nm. Addition of molecular oxygen to solutions of reduced chelated protoheme complexes yields product solutions with blue-shifted Soret bands that are characteristic of the Fe(III) complexes.

---

(58) Kadish, K. M.; Bottomley, L. A.; Beroiz, D. *Inorg. Chem.* **1978**, *17*, 1124.
(59) Fleischer, E. B.; Srivastava, T. S. *J. Am. Chem. Soc.* **1969**, *91*, 2403.
(60) Felton, R. H.; Linschitz, H. *J. Am. Chem. Soc.* **1966**, *88*, 1113.
(61) Kadish, K. M.; Morrison, M. M. *Bioinorg. Chem.* **1977**, *7*, 107.
(62) Nappa, M.; Valentine, J. S. *J. Am. Chem. Soc.* **1969**, *91*, 2403.

Table II. Redox Reactions for Metalloporphyrin Model Systems and Their $\mathrm{OH^-}$ and $\mathrm{O_2^-}$ Adducts in Dimethyl Sulfoxide (0.1 M Tetramethylammonium Perchlorate)[a]

A. Redox Couples for Porphyrin-Ring Reductions of $\mathrm{Zn^{II}TPP}$ and $\mathrm{Fe^{II}TPP}$ and Their $\mathrm{OH^-}$ Adducts

$$\mathrm{Zn^{II}TPP} + \mathrm{e^-} \underset{-1.28\ \mathrm{V}}{\overset{-1.34\ \mathrm{V}}{\rightleftharpoons}} \mathrm{Zn^{II}TPP^-} \underset{-1.68\ \mathrm{V}}{\overset{\mathrm{e^-},\ -1.74\ \mathrm{V}}{\rightleftharpoons}} \mathrm{Zn^{II}TPP^{2-}} \tag{5}$$

$$\mathrm{Fe^{II}TPP} + \mathrm{e^-} \underset{-1.13\ \mathrm{V}}{\overset{-1.19\ \mathrm{V}}{\rightleftharpoons}} \mathrm{Fe^{II}TPP^-} \underset{-1.58\ \mathrm{V}}{\overset{\mathrm{e^-},\ -1.64\ \mathrm{V}}{\rightleftharpoons}} \mathrm{Fe^{II}TPP^{2-}} \tag{6}$$

$$\mathrm{Zn^{II}TPP(OH)^-} + \mathrm{e^-} \underset{-1.36\ \mathrm{V}}{\overset{-1.51\ \mathrm{V}}{\rightleftharpoons}} \mathrm{Zn^{II}TPP^-} + \mathrm{OH^-} \underset{-1.70\ \mathrm{V}}{\overset{\mathrm{e^-},\ -1.76\ \mathrm{V}}{\rightleftharpoons}} \mathrm{Zn^{II}TPP^{2-}} + \mathrm{OH^-} \tag{7}$$

$$\mathrm{Fe^{II}TPP(OH)^-} + \mathrm{e^-} \underset{-1.15\ \mathrm{V}}{\overset{-1.45\ \mathrm{V}}{\rightleftharpoons}} \mathrm{Fe^{II}TPP^-} + \mathrm{OH^-} \underset{-1.58\ \mathrm{V}}{\overset{\mathrm{e^-},\ -1.64\ \mathrm{V}}{\rightleftharpoons}} \mathrm{Fe^{II}TPP^{2-}} + \mathrm{OH^-} \tag{8}$$

B. Reactions and Redox Couples for $\mathrm{Fe^{III}TPP^+}$, $\mathrm{Fe^{III}TPP\text{-}O\text{-}Fe^{III}TPP}$, and the $\mathrm{O_2^-}$ Adduct of $\mathrm{Fe^{II}TPP}$

$$\mathrm{Fe^{III}TPP^+} + \mathrm{e^-} \underset{-0.08\ \mathrm{V}}{\overset{-0.14\ \mathrm{V}}{\rightleftharpoons}} \mathrm{Fe^{II}TPP} \tag{9}$$

$$\mathrm{Fe^{III}TPP(OH)} + \mathrm{e^-} \underset{-0.68\ \mathrm{V}}{\overset{-0.74\ \mathrm{V}}{\rightleftharpoons}} \mathrm{Fe^{II}TPP(OH)^-} \tag{10}$$

$$\begin{tikzcd}
 & & \mathrm{Fe^{II}TPP^-} \\
\mathrm{Fe^{III}TPP\text{-}O\text{-}Fe^{III}TPP} + 2\mathrm{e^-} \arrow[r, "\mathrm{H_2O},\ -1.0\ \mathrm{V}"] & \mathrm{Fe^{II}TPP(OH)^-} + \mathrm{Fe^{II}TPP} + \mathrm{OH^-} \arrow[ur, "\mathrm{e^-},\ -1.2\ \mathrm{V}"] \arrow[dr, "-\mathrm{e^-},\ -0.68\ \mathrm{V}"'] & \\
 & & \mathrm{Fe^{III}TPP(OH)}
\end{tikzcd} \tag{11}$$

$$\mathrm{Fe^{II}TPP} + \mathrm{O_2^-} \rightarrow \mathrm{Fe^{III}TPP(O_2^{\,2-})^-} \tag{12}$$

$$\mathrm{Fe^{III}TPP(O_2^{\,2-})} + \mathrm{e^-} \underset{-1.04\ \mathrm{V}}{\overset{-1.34\ \mathrm{V}}{\rightleftharpoons}} \mathrm{Fe^{II}TPP(O_2^{\,2-})^{2-}} \xrightarrow{\mathrm{H_2O}} \mathrm{Fe^{II}TPP(O_2H)^-} + \mathrm{OH^-} \tag{13}$$

$$\mathrm{Fe^{II}TPP(O_2H)^-} + \mathrm{e^-} \underset{-1.41\ \mathrm{V}}{\overset{-1.51\ \mathrm{V}}{\rightleftharpoons}} \mathrm{Fe^{II}TPP^-} + \mathrm{HO_2^-} \underset{-1.58\ \mathrm{V}}{\overset{\mathrm{e^-},\ -1.64\ \mathrm{V}}{\rightleftharpoons}} \mathrm{Fe^{II}TPP^{2-}} + \mathrm{HO_2^-} \tag{14}$$

C. Redox Couples for $\mathrm{Fe^{III}PrH(ME)(Im)^+}$ and Its $\mathrm{OH^-}$ and $\mathrm{O_2^-}$ Adducts

$$\underbrace{\mathrm{Fe^{III}PrH(ME)^+}}_{\leftarrow \mathrm{Im}} + \mathrm{e^-} \underset{-0.09\ \mathrm{V}}{\overset{-0.21\ \mathrm{V}}{\rightleftharpoons}} \underbrace{\mathrm{Fe^{II}PrH(ME)}}_{\leftarrow \mathrm{Im}} \tag{15}$$

$$\underbrace{\mathrm{Fe^{II}PrH(ME)}}_{\leftarrow \mathrm{Im}} + \mathrm{e^-} \underset{-1.33\ \mathrm{V}}{\overset{-1.56\ \mathrm{V}}{\rightleftharpoons}} \mathrm{Fe^{II}PrH(ME)(Im)^-} \underset{-1.68\ \mathrm{V}}{\overset{\mathrm{e^-},\ -1.75\ \mathrm{V}}{\rightleftharpoons}} \mathrm{Fe^{II}PrH(ME)(Im)^{2-}} \tag{16}$$

$$\underbrace{\mathrm{Fe^{III}PrH(ME)(Im)(OH)}}_{\leftarrow \mathrm{Im}} + \mathrm{e^-} \underset{-0.80\ \mathrm{V}}{\overset{-0.82\ \mathrm{V}}{\rightleftharpoons}} \mathrm{Fe^{II}PrH(ME)(Im)(OH)^-} \tag{17}$$

$$\mathrm{Fe^{II}PrH(ME)(Im)(OH)^-} + \mathrm{e^-} \underset{-1.33\ \mathrm{V}}{\overset{-1.54\ \mathrm{V}}{\rightleftharpoons}} \mathrm{Fe^{II}PrH(ME)(Im)^-} + \mathrm{OH^-} \underset{-1.69\ \mathrm{V}}{\overset{\mathrm{e},\ -1.76\ \mathrm{V}}{\rightleftharpoons}} \mathrm{Fe^{II}PrH(ME)(Im)^{2-}} + \mathrm{OH^-} \tag{18}$$

$$\underbrace{\mathrm{Fe^{II}PrH(ME)}}_{\leftarrow \mathrm{Im}} + \mathrm{O_2^-} \rightarrow \mathrm{Fe^{III}PrH(ME)(Im)(O^{2-})^-} \tag{19}$$

$$\mathrm{Fe^{III}PrH(ME)(Im)(O_2^{\,2-})^-} + \mathrm{e^-} \xrightarrow{-1.48\ \mathrm{V}} \mathrm{Fe^{II}PrH(ME)(Im)(O_2^{\,2-})^{2-}} \xrightarrow{\mathrm{H_2O}} \mathrm{Fe^{II}PrH(ME)(Im)(O_2H)^-} + \mathrm{OH^-} \tag{20}$$

$$\mathrm{Fe^{II}PrH(ME)(Im)(O_2H)^-} \underset{-1.35\ \mathrm{V}}{\overset{-1.63\ \mathrm{V}}{\rightleftharpoons}} \mathrm{Fe^{II}PrH(ME)(Im)^-} + \mathrm{HO_2^-} \underset{-1.71\ \mathrm{V}}{\overset{\mathrm{e^-},\ -1.77\ \mathrm{V}}{\rightleftharpoons}} \mathrm{Fe^{II}PrH(ME)(Im)^{2-}} + \mathrm{HO_2^-} \tag{21}$$

D. Redox Couples for $\mathrm{Fe^{III}PrH(ME)(SC(O)Ph)}$ and Its -S^- and $\mathrm{O_2^-}$ Adducts

$$\mathrm{Fe^{III}PrH(ME)(SC(O)Ph)^+} + \mathrm{e^-} \underset{-0.17\ \mathrm{V}}{\overset{-0.23\ \mathrm{V}}{\rightleftharpoons}} \mathrm{Fe^{II}PrH(ME)(SC(O)Ph)} \tag{22}$$

$$\mathrm{Fe^{II}PrH(ME)(SC(O)Ph)} + \mathrm{e^-} \underset{-1.25\ \mathrm{V}}{\overset{-1.31\ \mathrm{V}}{\rightleftharpoons}} \mathrm{Fe^{II}PrH(ME)(SC(O)Ph)^-} \underset{-1.70\ \mathrm{V}}{\overset{\mathrm{e^-},\ -1.76\ \mathrm{V}}{\rightleftharpoons}} \mathrm{Fe^{II}PrH(ME)(SC(O)Ph)^{2-}} \tag{23}$$

$$\mathrm{Fe^{II}PrH(ME)(SC(O)Ph)} + 2\mathrm{OH^-} \rightarrow \underbrace{\mathrm{Fe^{II}PrH(ME)^-}}_{\leftarrow \mathrm{S}} + \mathrm{PhC(O)O^-} + \mathrm{H_2O} \tag{24}$$

$$\underbrace{\mathrm{Fe^{II}PrH(ME)^-}}_{\leftarrow \mathrm{S}} + \mathrm{e^-} \underset{-1.43,\ -1.28\ \mathrm{V}}{\overset{\mathrm{H_2O},\ -1.57\ \mathrm{V}}{\rightleftharpoons}} \mathrm{Fe^{II}PrH(ME)(SH)^-} + \mathrm{OH^-} \underset{-1.70\ \mathrm{V}}{\overset{\mathrm{e^-},\ -1.76\ \mathrm{V}}{\rightleftharpoons}} \mathrm{Fe^{II}PrH(ME)(SH)^{2-}} + \mathrm{OH^-} \tag{25}$$

Table II (*Continued*)

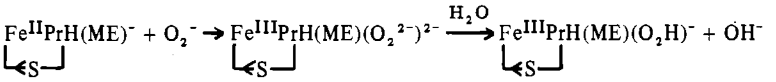

$$\mathrm{Fe^{II}PrH(ME)^- + O_2^- \rightarrow Fe^{III}PrH(ME)(O_2{}^{2-})^{2-} \xrightarrow{H_2O} Fe^{III}PrH(ME)(O_2H)^- + OH^-} \quad (26)$$

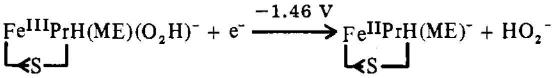

$$\mathrm{Fe^{III}PrH(ME)(O_2H)^- + e^- \xrightarrow{-1.46\ V} Fe^{II}PrH(ME)^- + HO_2^-} \quad (27)$$

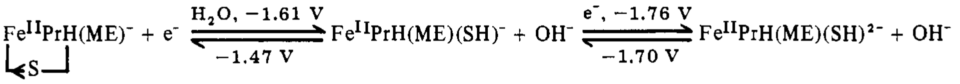

$$\mathrm{Fe^{II}PrH(ME)^- + e^- \underset{-1.47\ V}{\overset{H_2O,\ -1.61\ V}{\rightleftharpoons}} Fe^{II}PrH(ME)(SH)^- + OH^- \underset{-1.70\ V}{\overset{e^-,\ -1.76\ V}{\rightleftharpoons}} Fe^{II}PrH(ME)(SH)^{2-} + OH^-} \quad (28)$$

[a] The potentials represent the voltammetric peak potentials for a scan rate of 0.1 V s^{-1} and are vs. the SCE refernce electrode.

Magnetic Susceptibilities. The solid-phase magnetic moment of $Fe^{III}TPP^+$ is 5.92 μ_B; in Me_2SO solution its apparent value is 5.42 μ_B. The apparent solid-phase magnetic moment for $[Fe^{III}TPP]_2O$ is 2.43 μ_B (on the basis of the measured magnetic susceptibility and the assumption that the species is mononuclear in iron). The apparent magnetic moment for the product from the reaction of $Fe^{III}TPP^+$ plus at equiv of superoxide in Me_2SO is 4.46 μ_B (a mononuclear structure has been assumed). The addition of 2 equiv of superoxide yields a product with an apparent magnetic moment of 5.26 μ_B. The $Zn^{II}TPP$ complexes are diagmagnetic in the solid and solution phases.

Discussion and Conclusions

Redox Reactions of Iron Porphyrins. The cyclic voltammograms for the $Zn^{II}TPP$ and $Fe^{II}TPP$ porphyrins (Figure 1) are consistent with those for H_2TPP and $Zn^{II}TPP$ from previous studies[60,61] and confirm that the initial step of their reductive electrochemistry only involves the porphyrin ring system (Table II). Subsequent facile intramolecular electron transfer to the iron(II) may occur.

The addition of negatively charged axial ligand to either $Fe^{II}TPP$ or $Zn^{II}TPP$ causes the first porphyrin ring reduction to occur at more negative potentials. In the presence of OH^- the $Fe^{II}TPP$ reduction becomes less reversible but is analogous to that for the $Zn^{II}TPP$ system in the presence of excess base. Again, this is compelling evidence that the redox chemistry involves the porphyrin ring system and not the central metal, although changes in the axial ligand to the metal do cause changes in the electron distribution of the porphyrin ring. Because formation of $Zn^{I}TPP(OH)^{2-}$ is *not* a reasonable alternative, there is no rational reason to invoke direct electron transfer to the metal center for the FeTPP(OH) system when their reduction chemistry is virtually identical. The effect on the redox potentials due to axial ligation of $Zn^{II}TPP$ by OH^- clearly is not as great as that for the $Fe^{II}TPP$ system, but this only serves to indicate the extent of interaction of the metal with the electronic structure of the porphyrin. An alternative interpretation that invokes the Fe(I) state has been developed on the basis of Mössbauer data.[63] This would be consistent with a subsequent intramolecular electron transfer from the porphyrin ring to the metal.

Addition of an electron to $Fe^{II}TPP$ causes its molar absorptivity to change from 175 000 M^{-1} cm^{-1} at λ_{max} = 436 nm to 68 800 M^{-1} cm^{-1} at 394 nm and 75 000 M^{-1} cm^{-1} at λ_{max} = 418 nm for the reduction product, which represents a dramatic change in the electrostatics of the porphyrin ring. Furthermore, the α and β bands in the visible region are split into doublets due to the perturbation of the D_{4h} symmetry; the extra visible band at λ_{max} = 509 nm probably is due to a charge-transfer band or a spin-forbidden transition.

The porphyrin reduction peaks in the cyclic voltammograms for $(Fe^{III}TPP)_2O$ (Figure 3), $Fe^{III}PrH(ME)(Im)^+$ (Figure 4), and $Fe^{III}PrH(ME)(SC(O)Ph)^+$ (Figure 5) closely resemble those for $Fe^{III}TPP^+$ (Figure 2). Furthermore, the peak currents for each of the reductions are consistent with one-electron processes. Table II summarizes a set of self-consistent redox reactions for these systems as well as for $Zn^{II}TPP$ and $Fe^{II}TPP$ and their O_2^- and OH^- adducts.

Superoxide Adducts of Iron(II) Porphyrins. The electrochemical and spectroscopic results confirm that the product from the combination of $Fe^{III}TPP^+$ and 1 equiv of superoxide ion is a dioxygen adduct, $Fe^{II}TPP(O_2)$, which dissociates to $Fe^{II}TPP$ plus 1 equiv of molecular oxygen (Figure 2 and Table I). Reduction of the bound dioxygen of this adduct (Figure 2c) is facilitated through formation of an $Fe^{III}TPP(O_2{}^{2-})^-$ complex ($E_{p,c}$ = −0.73 V vs. SCE instead of −0.87 V for O_2 in a metal-free solution):[64]

$$Fe^{II}TPP(O_2) + e^- \rightleftharpoons Fe^{II}TPP(O_2{}^-)^- \rightarrow Fe^{III}TPP(O_2{}^{2-})^- \quad (29)$$

This reaction is favored by the hard acid–hard base interaction between iron(III) and the peroxo ligand. Reference to Figure 2c also indicates that the dioxygen adduct, $Fe^{II}TPP(O_2)$, is oxidized at +0.35 V vs. SCE:

$$Fe^{II}TPP(O_2) \rightarrow Fe^{III}TPP + O_2 + e^- \quad (30)$$

The superoxide adduct of $Fe^{II}TPP$ exhibits spectroscopic and electrochemical properties identical with those of the product of eq 29 (Figure 2 and Table I) and clearly exists as the $Fe^{III}TPP(O_2{}^{2-})$ species, which is in accord with a recent NMR study.[65] The electrochemistry of the latter can be represented by eq 13 and 14 of Table II. Trace water and other proton sources ultimately hydrolyze the bound $O_2{}^{2-}$ to form HO_2^-, which can act as a monodentate anion (with electrostatics that are equivalent to OH^-) to give $Fe^{III}TPP(O_2H)$. The initial oxidation peak at −0.1 V vs. SCE of Figure 2d appears to be due to this species:

$$Fe^{III}TPP(O_2H) \rightarrow Fe^{III}TPP + {}^1/_2H_2O_2 + {}^1/_2O_2 + e^- \quad (31)$$

The redox reactions for the $Fe^{III}PrH(ME)(Im)^+$ complex are similar to those for the $Fe^{III}TPP^+$ complex, with the first porphyrin-ring reduction for this chelated imidazole system shifted by −0.37 V relative to $Fe^{II}TPP$. This probably is due to axial binding of the iron center by the imidazole group (eq 15 and 16, Table IIC), which would increase the electron density on the metal and make reduction of the porphryrin ring more difficult.

Addition of hydroxide or superoxide to either the iron(III) or iron(II) forms of FePrH(ME)(Im) yields adducts that are analogous to those formed by the FeTPP complexes. Equations 17–21 of Table IIC summarize the reaction sequences.

The protoheme thioester complex, $Fe^{III}PrH(ME)(SC(O)Ph)^+$, exhibits redox chemistry that is analogous to that for the $Fe^{III}TPP^+$ complex (eq 22 and 23, Table IID). When the

---

(63) Reed, C. A. *Adv. Chem. Ser.* **1983**, *No. 201*, 333.

(64) Sawyer, D. T.; Chiericato, G.; Angelis, C. T.; Nanni, E. J., Jr.; Tsuchiya, T. *Anal. Chem.* **1982**, *54*, 1720.

(65) Shirazi, A.; Goff, H. M. *J. Am. Chem. Soc.* **1982**, *104*, 6318.

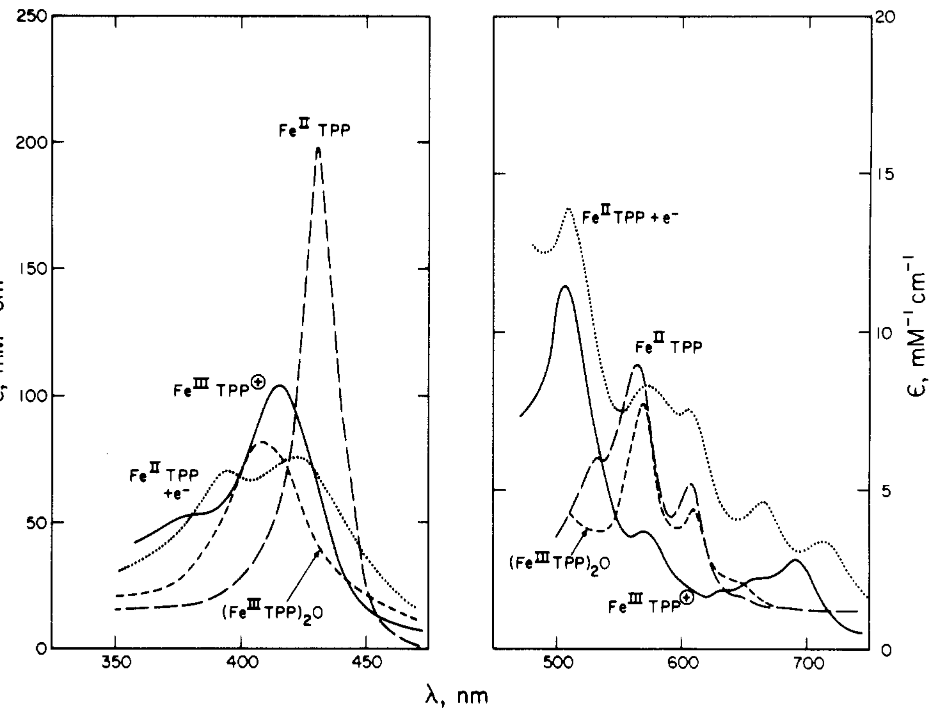

Figure 6. Absorption spectra in DMF (0.1 M TEAP) of $[Fe^{III}TPP]Cl$, $Fe^{II}TPP$ (from electroreduced $[Fe^{III}TPP]Cl$), $[Fe^{II}TPP + e^-]$ (from electroreduced $Fe^{II}TPP$), and $(Fe^{III}TPP)_2O$ (molar absorptivities are per porphyrin).

benzoyl protecting group is removed by base hydrolysis, the resulting thiolate binds to an axial site on iron. This conclusion is supported by the large negative shift in the potential for the first porphyrin-ring reduction ($E_{p,c} = -1.57$ V instead of -1.31 V). Addition of superoxide to the mercaptide complex, $\underline{S \rightarrow Fe}^{II}PrH(ME)^-$, yields an adduct with electrochemistry that is similar to that of the other model systems. However, the voltammograms are less well-defined, which probably is due to a more reactive peroxide moiety.

The results that are summarized in Table II illustrate the electrostatic effect of axial ligation by anions such as OH^-, O_2^-, and RS^- on the redox thermodynamics. There is clear evidence that the iron(II)–porphyrin centers are axially coordinated by OH^-, imidazole, and thiolate. When O_2^- is added to iron(II) porphyrin centers, an internal electron transfer occurs to give iron(III) peroxides. In the case of the $\underline{S \rightarrow Fe}^{III}PrH(O_2^{2-})^{2-}$ adduct, the system may represent an effective oxygenating agent.

The electrochemistry and redox processes of Figures 1–5 have been rationalized within the constraints of the iron(II) and iron(III) oxidation states. Thus, if the $Fe^{III}PrH(ME)(Im)(O_2^{2-})$ and $\underline{S \rightarrow Fe}^{III}PrH(O_2^{2-})^{2-}$ adducts are viable intermediates for oxidase and cytochrome P-450 monooxygenase chemistry, then invocation of exotic oxidation states such as iron(IV) and iron(V) is unnecessary.

Recent reports[66] propose mechanisms for cytochrome P-450 monooxygenase and peroxidase that are similar to the reactions of Table II. A critical step involves hydrolysis of an iron(III) peroxide complex, which is followed by hydroxylation of substrate. Other mechanisms invoke hydroperoxide formation via cytochrome P-450 chemistry with subsequent substrate hydroxylation.[67] Model studies are in progress to test the proposition that in situ generation of $Fe^{III}PrH(ME)(Im)(O_2^{2-})^-$ and $\underline{S \rightarrow Fe}^{III}PrH(O_2^{2-})^{2-}$ in the presence of substrate will promote peroxidase and monooxygenase reactions.

Acknowledgment. This work was supported by the National Science Foundation under Grants CHE82-12299 (D.T.S.) and CHE78-50003 (T.G.T.) and by the National Institutes of Health under Grant HL 13581 (T.G.T.).

Registry No. $Zn^{II}(TPP)$, 14074-80-7; $Fe^{II}(TPP)$, 16591-56-3; $[Zn^{II}(TPP)(OH)]^-$, 67820-15-9; $[Fe^{II}(TPP)(OH)]^-$, 54511-99-8; $[Fe^{III}(TPP)]^+$, 29484-63-7; $Fe^{III}(TPP)(OH)$, 25482-26-2; $Fe^{III}(TPP)$–O–$Fe^{III}(TPP)$, 12582-61-5; $[Fe^{III}(TPP)(O_2^{2-})]^-$, 87803-92-7; $[Fe^{II}(TPP)(O_2^{2-})]^{2-}$, 87803-93-8; $[Fe^{II}(TPP)(O_2H)]^-$, 87803-94-9; $[Fe^{III}(PrH(ME)(Im))]^+$, 87803-95-0; $Fe^{II}(PrH(ME)(Im))$, 72177-45-8; $[Fe^{II}(PrH(ME)(Im))]^-$, 87803-96-1; $[Fe^{II}(PrH(ME)(Im))]^{2-}$, 87803-97-2; $Fe^{III}(PrH(ME)(Im))(OH)$, 87803-98-3; $[Fe^{II}(PrH(ME)(Im))(OH)]^-$, 87803-99-4; $[Fe^{III}(PrH(ME)(Im))(O_2^{2-})]^-$, 87804-00-0; $[Fe^{II}(PrH(ME)(Im))(O_2^{2-})]^{2-}$, 87804-01-1; $[Fe^{III}(PrH(ME)(SC(O)Ph))]^+$, 87804-03-3; $Fe^{II}(PrH(ME)(SC(O)Ph))$, 87804-04-4; $[Fe^{II}(PrH(ME)(SC(O)Ph))]^-$, 87804-05-5; $[Fe^{II}(PrH(ME)(SC(O)Ph))]^{2-}$, 87804-06-6; $[Fe^{II}(PrH(ME)(S))]^-$, 87804-07-7; $[Fe^{II}(PrH(ME)(SH))]^-$, 87804-08-8; $[Fe^{II}(PrH(ME)(SH))]^{2-}$, 87804-09-9; $[Fe^{III}(PrH(ME)(S))(O_2^{2-})]^{2-}$, 87804-10-2; $[Fe^{III}(PrH(ME)(S))(O_2H)]^-$, 87828-75-9; $Fe^{III}(TPP)Cl$, 16456-81-8; $Fe^{III}(PrH(ME)(Im))Cl$, 72177-42-5; $Fe^{III}(PrH(ME)(SC(O)Ph))Cl$, 87804-11-3; Me_2SO, 67-68-5.

---

(66) (a) Sligar, S. G.; Kennedy, K. A.; Pearson, D. C. *Proc. Natl. Acad. Sci. U.S.A.* **1980**, *77*, 1240. (b) White, R. E.; Sligar, S. G.; Coon, M. J. *J. Biol. Chem.* **1980**, *255*, 11108.

(67) Blake, R. C.; Coon, M. J. *J. Biol. Chem.* **1981**, *256*, 12127.